Chemical Engineering Journal 471 (2023) 144310

Contents lists available at ScienceDirect

Chemical Engineering Journal

journal homepage: www.elsevier.com/locate/cej

Phosphorus recovery and resource utilization from phosphogypsum leachate via membrane-triggered adsorption and struvite crystallization approach

Xinping Hu [a,b], Jingfu Wang [a,b,*], Fengxue Wu [a], Danhao Li [a,d], Jiaojiao Yang [a,b], Jingan Chen [a,b], Jiaxin Liang [c], Xiangyang Lou [c], Hong Chen [c,*]

[a] State Key Laboratory of Environmental Geochemistry, Institute of Geochemistry, Chinese Academy of Sciences, Guiyang 550081, China
[b] University of Chinese Academy of Sciences, Beijing 100049, China
[c] School of Environmental Science and Technology, Southern University of Science and Technology, Shenzhen 518055, China
[d] State Key Laboratory of Eco-hydraulics in Northwest Arid Region of China, Xi'an University of Technology, Xi'an 710048, China

ARTICLE INFO

Keywords:
Phosphogypsum
Phosphorus recovery
ZrO_2 membrane
Struvite crystallization

ABSTRACT

Phosphorus pollution from phosphogypsum (PG) leachate has caused severe problems in the water environment and ecology. Efficient phosphate recovery and resource utilization techniques are crucial as they can aid the phosphorus pollution problem and recover the scarcity of phosphorus resources. Herein, we developed a highly efficient phosphorus recovery strategy from PG leachate by integrating the ZrO_2 membrane-triggered adsorption technique with the struvite crystallization process. More than 89.23% of the phosphorus anions in the PG leachate can be recovered via membrane-triggered adsorption. With the concentrated phosphate anions washed from membrane adsorption, the phosphate anions can be further employed for struvite crystallization, and an overall phosphorus recovery efficiency of 59.36% can be achieved. The obtained fine struvite product is of high purity, with $NH_4MgPO_4{\cdot}6H_2O$ weight ratio of up to 89.83%. The novel strategy developed here demonstrates a green and sustainable strategy toward phosphorus recovery from the PG or PG-polluted groundwater or surface water leachate, which could be applied to practical phosphorus recovery and struvite fertilizer production. The commercialization of this strategy will shed light on the emergency PG pollution control at the YangtzeRiver upstream area.

1. Introduction

Phosphorus is a critical fertilizer extensively consumed in agriculture [1]. With the continuous growth of the global population, phosphorus fertilizer scarcity has spread worldwide [2]. Natural mining from the phosphate rock is the primary source of obtaining phosphorus fertilizer, while with the rapid consumption rate worldwide, the phosphate rock reserves are depleted rapidly [3]. It is urgent to find new sources of phosphorus or recycle and reuse the widely spread phosphorus anions in surface water or groundwater.

PG is a solid waste byproduct introduced in phosphoric acid production. 4.5–5.5 tons of PG are produced for one ton of phosphoric acid production [4,5]. Statistics data shows that there are currently more than 6 billion tons of PGs accumulated worldwide, with an annual growth of ~ 280 million tons [6]. Although massive PG has been produced, less than 15% has been reutilized globally [7]. Most of the PG are deposited in slag fields, which not only occupy large amounts of land but can also cause severe water pollution and eutrophication problem in rivers, lakes, and reservoirs as 0.5–0.7% weight percentage of phosphorus within PG can generate hazardous leachate from the solid waste and then enter into the groundwater and surface water [8,9].

One of the areas with severe and emergency phosphorus contamination problems is the Yangtze River Basin in China [10]. Abundant phosphorus anions present in PG, in speciation of $Ca(H_2PO_4)_2{\cdot}2H_2O$, $CaHPO_4{\cdot}2H_2O$, $Ca_3(PO_4)_2$, and residual phosphoric acid (H_3PO_4), significantly contributed to the eutrophication of water bodies, originated from the low resource utilization rate of PG [11,12]. As the local government implemented the policy of "no PG consumption, no

* Corresponding authors at: State Key Laboratory of Environmental Geochemistry, Institute of Geochemistry, Chinese Academy of Sciences, Guiyang 550081, China (J. Wang).
E-mail addresses: wangjingfu@vip.skleg.cn (J. Wang), chenh3@sustech.edu.cn (H. Chen).

https://doi.org/10.1016/j.cej.2023.144310
Received 12 March 2023; Received in revised form 14 June 2023; Accepted 21 June 2023
Available online 29 June 2023

phosphate acid production" in recent years, the amount of PG consumed from the landfill directly limited the local companies' phosphoric acid productivity [13]. Green and resource utilization of PG solid waste, together with its leachate, is vital to the sustainable development of the phosphorus industry.

Historically, pretreatment techniques like PG washing, pickling, calcination, and lime neutralization can remove or stabilize the phosphorus anions within PG, while the enormous chemicals, energy consumption, and environmental side effects prevent the broad application of this technique. Biological, adsorption, chemical precipitation, crystallization, and other processes tend to be greener approaches to address this problem [14]. Especially for the adsorption technique, zirconium-based materials show great adsorption capacity and outperform other materials [15,16,17]. It is feasible to employ ZrO_2 to recover phosphorus from various water bodies containing complex compositions.

In this work, PG samples from three large-scale slag sites in Southwest China have been collected. Integrating membrane-triggered adsorption with struvite crystallization, a highly efficient phosphorus removal and recovery strategy has been developed for treating PG leachate. The detailed mechanism of membrane-triggered adsorption and precipitate-introduced crystallization process has been illustrated down to the atomic scale. The design ensures the efficient removal of phosphorus from PG leachate and demonstrates a novel and green approach to phosphorus recovery and resource utilization. The current method shows great potential for large-scale application of phosphorus recovery and struvite fertilizer production from the PG polluted groundwater or surface water.

2. Materials and methods

2.1. Materials

The details of chemicals used in this work are documented in the Supporting Information (Text S1). All the PGs used in this study came from the PG slag fields in Guiyang, China. The specific sampling points are shown in Fig. S1. The chemical composition and morphology of PG were analyzed. The results are shown in Fig. S2 and Table S1. The differences in origin and storage years lead to variation in the chemical composition of PG. The phosphorus content in PG is 0.30–0.63%.

2.2. ZrO_2 membrane fabrication

The ZrO_2 membrane is fabricated according to the following recipe. 25 g of zirconyl chloride octahydrate ($ZrOCl_2{\cdot}8H_2O$) was weighed and added into a 1 L beaker. 600 mL of deionized water was added under continuous stirring with a glass rod until the $ZrOCl_2{\cdot}8H_2O$ was completely dissolved. The mixed solution was titrated to pH = 7.0 ± 0.1 with 25% ammonia solution and aged for 24 h. The as-formed solid product was separated via centrifugation and rinsed three times with deionized water to remove the residue chloride ions with the solid product. The final product was then dried in a 105°C oven for 4 h and ground into fine powders. The powdery hydrated zirconia was successfully prepared after passing through a 100-mesh sieve.

14.25 g acrylamide and 0.75 g N, N′-methylene bis (acrylamide) were weighted and dissolved in deionized water to prepare a 50 mL stock gel. 3.6 mL stock gel and 3.6 mL deionized water were placed in a glass beaker, 0.06 g of zirconia powder, 70 μL of 10% (w/v) ammonium persulfate and 10 μL of tetraethylethylenediamine were added, respectively, while stirring was maintained to mix and degas. Then the mixture was injected into a 5 cm × 5 cm glass splint with a thickness of 0.4 mm, and stood for 30 min to allow the zirconia powder to settle to one side of the film by gravity. The entire glass splint was then baked in an oven at 40°C for 30 min and soaked in deionized water for 5 h [18]. 0.06 g of zirconia powder has been loaded on the membrane via this process. A 3.14 cm^2 ZrO_2 membrane has been successfully fabricated with a thickness of 0.4 mm.

2.3. Phosphorus extraction and leachate preparation

All leachate preparation experiments in this work were performed at 25 ± 1℃. 1.00 g of Jiaoyishan (JYS), Guwang (GW), Baiji (BJ) were weighted for each sample, while solutions with pH range of 0–12 were prepared mixing deionized water, 1 M HCl and 1 M NaOH solution in different proportions. 10 mL extraction solvent with pH = 0–12, deionized water (pH = 5.34), and 10–80 mL of 1 M HCl solution were used to extract PG phosphorus (PG-P) to study the optimal extraction solvent and liquid–solid ratio, respectively. 40, 70, 50 mL 1 M HCl solution was used to extract the phosphorous anions from JYS, GW, BJ PGs with a varied time of 10–60 min to optimize the extraction time. The phosphate content was determined via a molybdenum blue method after the samples were shaken for 2 h and stood for 5 min [19], with the supernatant passed through a 0.45 μm cellulose acetate membrane.

2.4. Adsorption experiments

All adsorption experiments were performed at 25 ± 1℃. 200, 400, 600, 800, 1000, 1500 mg/L phosphate solution (pH = 4.6 ± 0.1) and PG leachate were prepared, while each sample was added with a piece of 3.14 cm^2 ZrO_2 membrane. Adsorption kinetics and isotherms were investigated in batch experiments, whose principles and formulas are documented in Text S2. Kinetic data were measured at three initial phosphorus concentrations (200, 400, and 600 mg/L), and the time intervals were set to 0.5, 1, 2, 4, 8, 12, 16, and 24 h. The isotherms were determined under six initial phosphorus concentrations (200, 400, 600, 800, 1000, 1500 mg/L), with temperatures of 25, 35, and 45°C. The shaking time has been set to be 24 h. In addition, the ZrO_2 membrane was added to 10 mL 600 mg/L phosphate solution with pH = 0–12 and shaken for 24 h to study the optimal adsorption pH. ZrO_2 membranes were added into PG leachate for 0.5, 1, 2, 4, 8, 12, 16, and 24 h to study the optimal adsorption time. The supernatant was passed through a 0.45 μm cellulose acetate filter to determine the phosphate content with the molybdenum blue method after the samples were shaken and stood for 5 min except for specific reaction time.

2.5. Desorption and recycle experiments

At 25 ± 1°C, ZrO_2 membranes that reached adsorption equilibrium in PG leachate were prepared. The ZrO_2 membrane loaded within phosphorus anions contained solution under different pH values to optimize the best desorption condition. After that, 1 M NaOH solution was used to desorb phosphorus on the ZrO_2 membrane for 0, 1, 2, 4, 8, 12, 16 and 24 h to optimize desorption time. The recycling experiments were carried out with the adsorption and desorption experiments periodically. The recycling experiments were terminated when the phosphorus adsorption efficiency was less than 50% of its original capacity. The supernatant was passed through a 0.45 μm cellulose acetate membrane to determine the phosphate content after the samples were shaken and stood for 5 min except for a specific reaction time.

2.6. Struvite crystallization experiments

All the struvite crystallization experiments were performed at 25 ± 1°C. To study the reaction mechanism of the struvite crystallization process, simulated MAP crystallization experiments were performed with 0.1 M KH_2PO_4, $MgCl_2{\cdot}6H_2O$, NH_4Cl solution, respectively. During this process, 1 M NaOH was used adjust the pH to 7.23–11.02. KH_2PO_4, $MgCl_2{\cdot}6H_2O$ and NH_4Cl solution were added in a 50 mL beaker in sequence, with the P: N: Mg ratio controlled to be 1:1:1. 25 g, 15 g, and 20 g of JYS, GW, and BJ PG were used to prepare leachate referring to the best extraction strip, and 25, 15, and 20 sheets of ZrO_2 membrane with an area of 3.14 cm^2 were added to adsorb phosphorus. 100 mL of 1 M NaOH was used for phosphorus desorption to achieve an enriched solution. For the struvite crystallization with practical water, with the

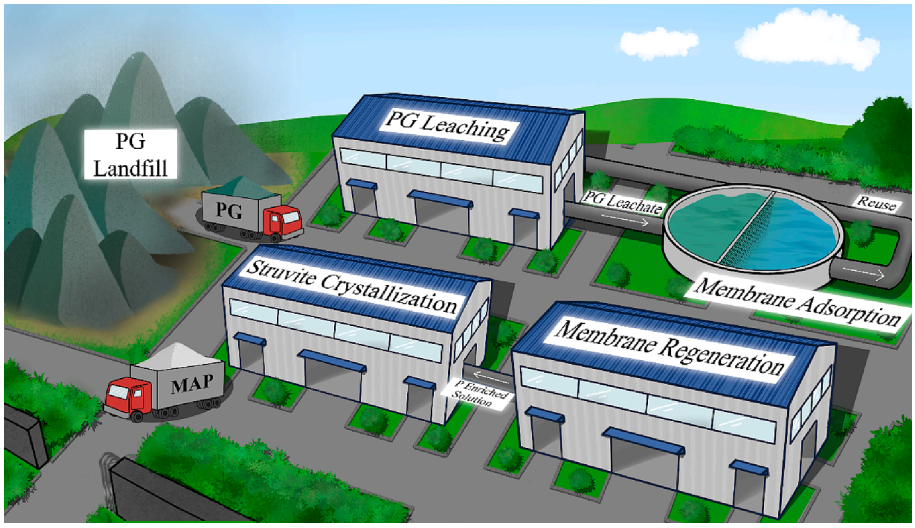

Fig. 1. Schematic illustration of the integrated membrane-triggered adsorption combining struvite crystallization concept for phosphorus recovery from PG leachate.

phosphorus desorbed from ZrO_2 adsorption, 10 mL 0.019, 0.017, 0.012 M $MgCl_2{\cdot}6H_2O$ and NH_4Cl solution were added in 10 mL BJ, JYS, GW PG eluent, respectively. The P: N: Mg ratio was controlled to be 1:1:1. The pH was adjusted to 8.02–10.97. Within this pH window, colorless crystals have been precipitated in the solution, whose purity calculation refers to Text S3. The solid liquid was separated via decantation after crystallization.

2.7. Material characterization

The pH value of the solution was measured with a pH meter (Fivego F2, Mettler Toledo, Germany). The microscopic morphology and elemental compositions of all the solid-state materials were studied with a field emission scanning electron microscope (SEM, JSM-7800F) equipped with an energy-dispersive X-ray spectrometer (EDS, EDAX

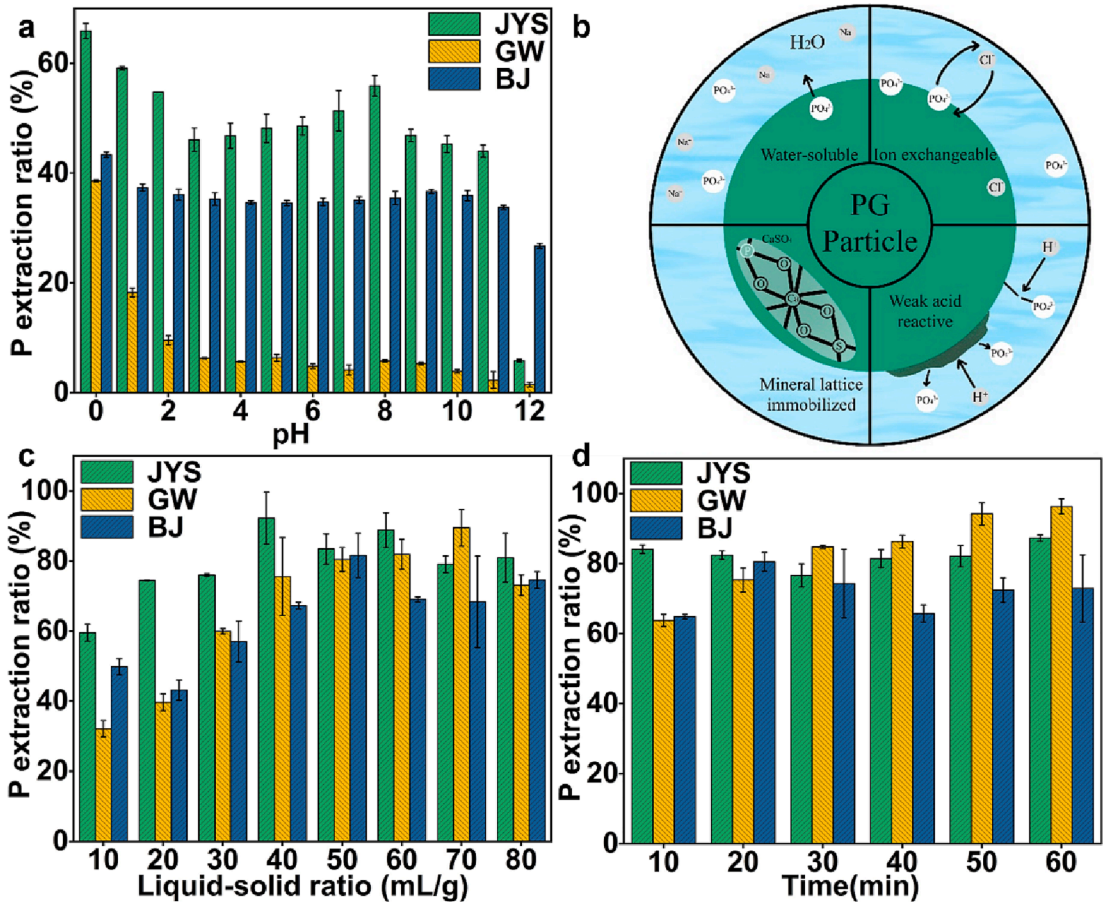

Fig. 2. Effects of different conditions on PG-P extraction. Influences of (a) Variety of pH extractants (Liquid-solid ratio:10; Extraction time:120 min); (b) Different forms of phosphorus ions in PG; (c) Liquid-solid ratio (Extractant:1 M HCl solution; Extraction time: 120 min); (d) Extracting time (Extractant:1 M HCl; liquid–solid ratio of JYS, GW, BJ were set to 40, 50 and 70, respectively).

TEAM Apollo XL). Quantitative elements analysis of all samples was determined with the X-ray fluorescence spectrometer (XRF, Axios mAX). Inductively coupled plasma mass spectrometry (ICP-MS, ELMENT) was used to analyze the trace elements and heavy metals in all samples. The anions in all the samples were determined by anion chromatography (ICS-90) and inductively coupled plasma optical emission spectrometer (ICP-OES, Vista MPX), respectively. The crystallographic phases of all samples were analyzed by a powder crystal X-ray diffractometer (XRD, Empyream, Netherlands). The valence states of all the surface elements were determined by X-ray photoelectron spectroscopy (XPS, Thermo Scientific Nexsa). The bond vibration of all the samples has been carried out with the Thermo Scientific Nicolet 6700 Fourier transform infrared spectroscopy (FTIR, America).

3. Results and discussion

3.1. Concept of current work

Traditional phosphorous recycling techniques either focused on the adsorption or precipitation of phosphorous anions, which is hard to be used for low-concentration phosphorous recovery from complex PG leachate. Herein, we integrate the ZrO_2 membrane-triggered phosphorous anions adsorption technique with the struvite crystallization approach for phosphorus recovery. Via this approach, the phosphorous anions in the PG leachate can be directly resource utilized and turned into valuable struvite products. Four distinct steps are compulsory to employ this concept for phosphorous anions recycling from PGs: 1) Leachate origin; 2) ZrO_2 membrane triggered phosphorus adsorption; 3) Phosphorus anions enrichment; 4) Struvite crystallization. Fig. 1 shows the overall processes within this concept. Among all four steps, the phosphorous anions adsorption from the PGs solution and the struvite crystallization steps are crucial for achieving highly efficient phosphorus recovery.

3.2. Phosphorus leachate origination

The phosphorus leachate can be originated in different ways. The leachate from long-term landfilled spots can be directly collected at downstream of the landfill point. As some of the PG landfilled points suffers severe phosphorous leaching problem, a large amount of phosphorus anions are washed by the rainwater and enter into surface water or groundwater to form phosphorus leachate with different phosphorus concentrations. In our study, to get a consistent understanding of phosphorus recovery from PG leachate, fresh PGs have been used in the study. Thus three leachates have been prepared in the lab. Under this circumstance, the composition of PG leachate has been extensively affected by factors like extraction solvent conditions, liquid–solid ratio, extraction time, and temperature. In this study, from a cost-effective point of view, we carefully evaluate the effects of three factors: extraction solvent conditions, liquid–solid ratio, and extraction time.

3.2.1. Extraction solvent conditions

From a cost point of view, water is the cheapest solvent frequently used for phosphorus extraction. While the conditions, such as acidity, reactivity, and pH values in water, are crucial for extracting phosphorus anions from PG. In natural landfill sites, the extraction solvent is rainwater with weak acidity. After long-term flushing by rainwater, the phosphorus anions in landfill sites can be effectively transported into the leachate. In the lab experiments, we are interested in effectively recovering the residue phosphorus anions within PG with low costs. Typical inorganic water solutions with a low economic cost, including HCl aqueous solution and deionized water, have been employed as the extraction solvents. The HCl can provide H^+ to react with the surface OH^- group in order to release the surface-bonded phosphorous anions. In previous reports, H_2SO_4, HNO_3, etc. had also been frequently used for phosphorous extraction from PG [20]. While considering extraction efficiency and cost, we focus more on HCl in this study. As shown in Fig. 2a, we carefully evaluate the extraction efficiency of variety of aqueous solutions with pH in the range 0–12. We found that the phosphorus extraction efficiency with deionized water and formulated solution at pH = 5 is similar. Herein, deionized water (pH = 5.34) can be directly used for phosphorus extraction similar to the aqueous solution with a corresponding pH value of 5. Compared to deionized water, the extraction efficiency with 1 M HCl is significantly enhanced for all the PGs sampled from three different locations. In these three PGs, the tendency of water-soluble and ion-exchangeable phosphorous anions is in line with JYS > BJ > GW, suggesting a diversity ion exchange difficulty with the PGs from different locations. Further evaluating the pH-dependent extraction efficiency with HCl aqueous solution, it can be seen that the exchangeable Cl^- concentrations and reactive H^+ concentrations in the extraction solvents are increased with the decreasing pH values. A significant amount of phosphorous extraction efficiency has been achieved, primarily when 1 M HCl aqueous solution has been employed for PG washing. These results indicated that the proton in the HCl solution could further enhance the phosphorous extraction efficiency with a final extraction rate of 65.88 ± 1.39%, 38.60 ± 0.23%, 43.36 ± 0.51% for the PGs from JYS, GW and BJ. The residue of unextractable phosphorus anions may be immobilized within different minerals or PG lattices and inert to weak acid, thus it can not be extracted even in 1 M HCl solution. These results suggest that the phosphorous anions might be preserved within PG in four states, including the water-soluble, ion exchangeable, weak acid reactive, and mineral lattice immobilized, as shown in Fig. 2b. Here, as the phosphorus recovery efficiency is high enough, considering the increased cost with higher HCl concentrations, only 1 M HCl solution is used in later studies.

3.2.2. Liquid-solid ratio

An optimal liquid–solid balance is crucial for efficiently extracting the phosphorous anions to obtain a high-concentration leachate. The optimal liquid–solid ratio is significantly different for PG sampling from three locations. As shown in Fig. 2c, by using 1 M HCl as extraction solvent, with the liquid–solid ratio increased, the phosphorus extraction ratio increased gradually. The phosphorus extraction ratios of JYS, GW, and BJ began to decline when the liquid–solid ratio exceeded 40, 70, and 50, respectively. Under the optimal liquid–solid ratio, the phosphorus extraction ratio reached 92.28 ± 7.39%, 89.53 ± 5.20% and 81.62 ± 6.29%, respectively.

3.2.3. Extraction time

To understand the time-dependent leaching behavior of PG, the time-dependent extraction efficiency has been evaluated. As shown in Fig. 2d, BJ reached the maximum phosphorus extraction ratio in 20 min. The corresponding extraction efficiency was 80.50 ± 2.69%. JYS and GW reached their maximum phosphorus extraction ratio of 87.29 ± 0.91%, and 96.33 ± 2.15% in 60 min (Fig. 2d). This may be attributed to the different proportion of solid bonding forces between phosphorus anions with the corresponding mineral composites inside PG. To maximize the extraction rate in all these three PGs, the optimal extraction time has been set to 1 h.

3.3. ZrO_2 membrane triggered phosphorus adsorption

ZrO_2 has been extensively reported as an effective material for phosphorus adsorption [21,22,23]. With this regard, we fabricated the ZrO_2 powder into a membrane and employed it for phosphorus adsorption. Benefiting from the strong affinity between the ZrO_2 membrane and phosphorus anions, the phosphorus anions within the PG leachates can be effectively uptaken. Furthermore, the adsorption process is heavily influenced by pH, temperature, time, etc [18]. Here we focused on the two most essential factors in the future industrial process, pH and time, to understand their effects on phosphorus adsorption.

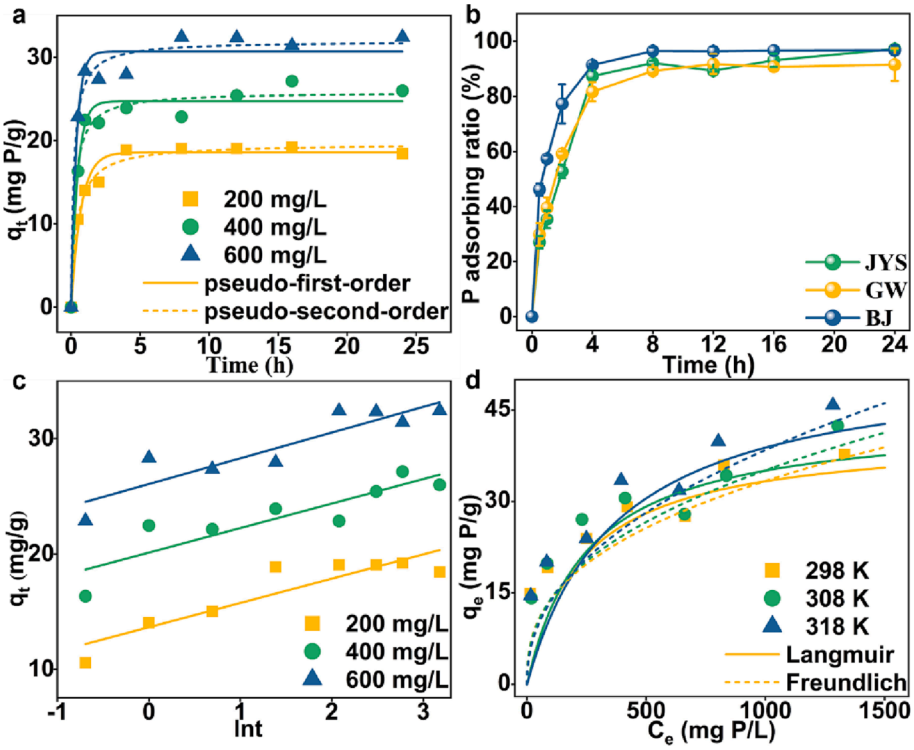

Fig. 3. Adsorption Kinetics and thermodynamics of ZrO_2 membrane (n = 3). (a) pseudo-first-order and pseudo-second-order models. (b) Time-dependent P extraction ratio from ZrO_2 membrane. (c) Elovich models. (d) Langmuir and Freundlich models.

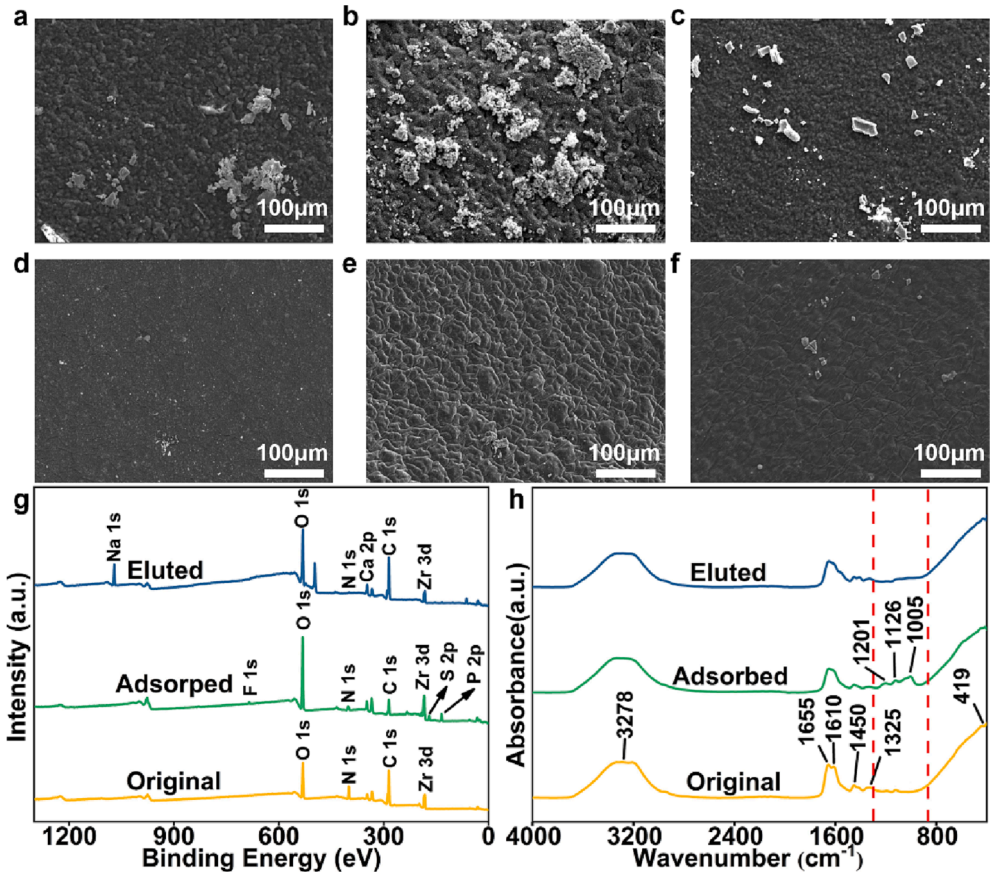

Fig. 4. Characterization of ZrO_2 membrane. After adsorption in (a) BJ, (b) JYS, (c) GW leachate. After Desorption for ZrO_2 membrane from (d) BJ, (e) JYS, (f) GW leachate. (g) XPS surveys and (h) FTIR spectra of original, adsorbed and desorbed ZrO_2 membrane.

*pH 14.0 represents 1 M NaOH solution.

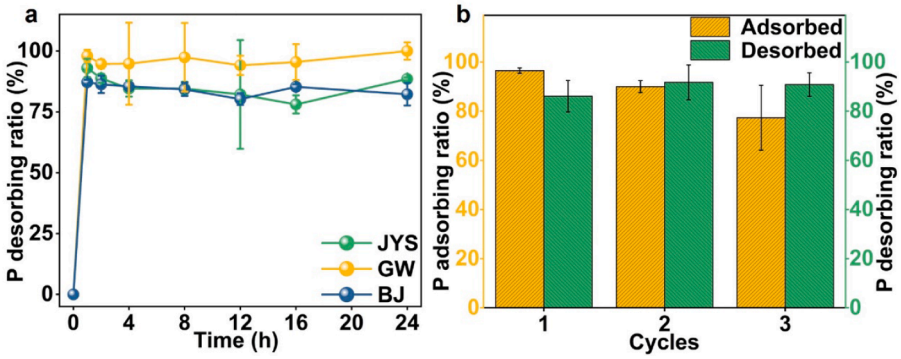

Fig. 5. P extraction from ZrO_2 membrane. (a) Adsorption performance of the regenerated ZrO_2 membrane; (b) Recycling performance of ZrO_2 membrane.

3.3.1. *Effect of pH*

The pH can determine the proton concentration within the solution, thereby significantly influencing the maximum adsorption capacity. As shown in Fig. S3, within pH of 0.42–2.60, the maximum adsorption ratio is 51.34 ± 2.72%; with the pH increased to 3.65–7.37, the maximum adsorption ratio is reduced to 38.50 ± 0.27%; further increased the pH to 8.45–10.48, the maximum adsorption ratio is reduced to 28.71 ± 3.39%; at a high pH of 11.37–12.41, the maximum adsorption ratio dropped to 18.06 ± 3.50%. The optimal adsorption pH of the ZrO_2 membrane is 0.42–2.60, which is also an optimal pH for phosphorus anions leaching from PG, indicating that there is no special requirement to pretreat the PG leachate. The PG leachate obtained from the HCl leaching process can be directly utilized in ZrO_2 membrane adsorption.

3.3.2. *Effect of adsorption time*

To evaluate the adsorption equilibrium time of ZrO_2 membrane, different concentrations (200, 400, 600 mg/L) of the artificial phosphorous solution have been used for the adsorption experiments. As shown in Fig. 3a, the fitting results of the pseudo-second-order kinetic model indicate that the adsorption equilibrium time of the ZrO_2 membrane is 8 h, which is consistent with the results obtained in the natural PG wastewater (Fig. 3b). Based on these results, it can be concluded that the adsorption equilibrium time of ZrO_2 membrane is not affected by the concentration in phosphorus solutions with concentrations lower than 600 mg/L. Further fitting the data with different theoretic models (Fig. 3a and Fig. 3c), a pseudo-second-order kinetic model (R^2 = 0.974–0.987) can be used to fit the data as shown in Table S2 better than the pseudo-first-order kinetic model (R^2 = 0.964–0.970) and Elovich model (R^2 = 0.448–0.470), which indicates that the adsorption of phosphate anions by ZrO_2 membrane is mainly controlled by chemical adsorption [24]. Referring to these results, the adsorption time for all the PG leachates has been set to 8 h. Within this period, the extraction efficiency of JYS, GW, BJ by ZrO_2 membrane can reach up to 92.14 ± 0.78%, 89.23 ± 1.31% and 96.49 ± 1.23%, respectively.

3.3.3. *Isotherm analysis of the adsorption behavior*

To understand the thermodynamics during the adsorption process, the Freundlich and Langmuir model has been used to fit the adsorption curves, as shown in Fig. 3d and Table S3. Based on the fitting results, it is obvious that the Freundlich model (R^2 = 0.969–0.982) is better fit than the Langmuir model (R^2 = 0.922–0.939). The fitting results suggested that the phosphorus adsorption process of ZrO_2 membrane is a quickly occurring adsorption-complexation process (0.5 less than 1/n less than 1)[25].

3.3.4. *Status of phosphate on ZrO_2 membrane after adsorption*

To understand the phosphate status after adsorption, the ZrO_2 after 8 h of adsorption in three different PG leachates has been characterized with SEM and EDS. It can be seen from the SEM-EDS results that colloidal particles with P as the main component have been uniformly distributed on ZrO_2 membrane (Fig. 4a-c and Fig. S4). After washing the membrane with 1 M NaOH solution, a cleaner membrane with Zr, O as the main components, with minor elements of Na and Ca is presented as shown in Fig. 4d-f. The membrane can be well regenerated, which indicates good reusability of the ZrO_2 membrane.

Table 1
Phosphorus recovery with different pH eluents.

pH	Phosphorus recovery ratios (%)		
	JYS	GW	BJ
1.00	7.38 ± 4.95	19.78 ± 5.36	11.67 ± 0.83
2.00	4.27 ± 0.27	20.91 ± 1.47	9.68 ± 1.30
3.00	3.31 ± 0.58	17.02 ± 2.01	11.57 ± 1.40
4.00	4.76 ± 1.72	24.69 ± 9.51	9.56 ± 1.67
5.00	6.04 ± 2.98	25.28 ± 7.12	9.56 ± 0.21
6.00	3.75 ± 2.03	27.52 ± 14.59	14.67 ± 3.88
7.00	5.61 ± 3.95	26.81 ± 6.05	8.60 ± 0.79
8.00	3.75 ± 0.62	24.38 ± 8.00	12.15 ± 4.36
9.00	7.64 ± 6.57	36.49 ± 8.41	10.83 ± 1.06
10.00	3.29 ± 0.59	28.35 ± 8.82	17.97 ± 9.41
11.00	6.53 ± 4.31	23.56 ± 6.24	14.85 ± 7.40
12.00	8.67 ± 4.44	24.22 ± 2.68	12.27 ± 1.64
14.00*	92.13 ± 1.58	97.86 ± 3.90	92.95 ± 10.22

* pH 14.0 represents 1 M NaOH solution.

To further understand the chemical speciation of the adsorbed phosphate components, XPS and FT-IR spectra have been employed to analyze the distinct chemical group within ZrO_2 membrane after phosphate adsorption. As shown in Fig. 4g, Zr, O, P, F, and S were observed within the membrane after phosphate adsorption, which proved that phosphorus was successfully adsorbed onto ZrO_2 membrane. According to the reported results, when employing ZrO_2 for anions adsorption, the affinity between ZrO_2 and anions follows the below ordering: $I^- \approx Br^- < ClO_4^- < Cl^- < NO_3^- < SO_4^- < F^- \approx C_2O_4^{2-} \approx PO_4^{3-} < CO_3^{2-} < OH^-$ [26]. With this regard, phosphorus can be selectively adsorbed on the membrane even under acidic conditions. Only minor sulfate and fluoride anions within leachate have been co-adsorbed (Fig. S5). Moreover, FTIR spectra have also been collected, as shown in Fig. 4h. Specific bands located at 1201 and 1126 cm^{-1} are observed, corresponding to the characteristic vibration of $H_2PO_4^-$ [27]. Furthermore, a band at 1005 cm^{-1} is also present. These results indicate that the phosphate anions within the leachate have been successfully adsorbed on the ZrO_2 membrane.

3.3.5. *Desorption and recycling of ZrO_2 membrane*

To recycle the phosphorous anions from ZrO_2 membrane, 1 M NaOH solution was used to extract the phosphorus anions from the membrane. As shown in Fig. 5a, the membranes used to adsorb phosphate anions

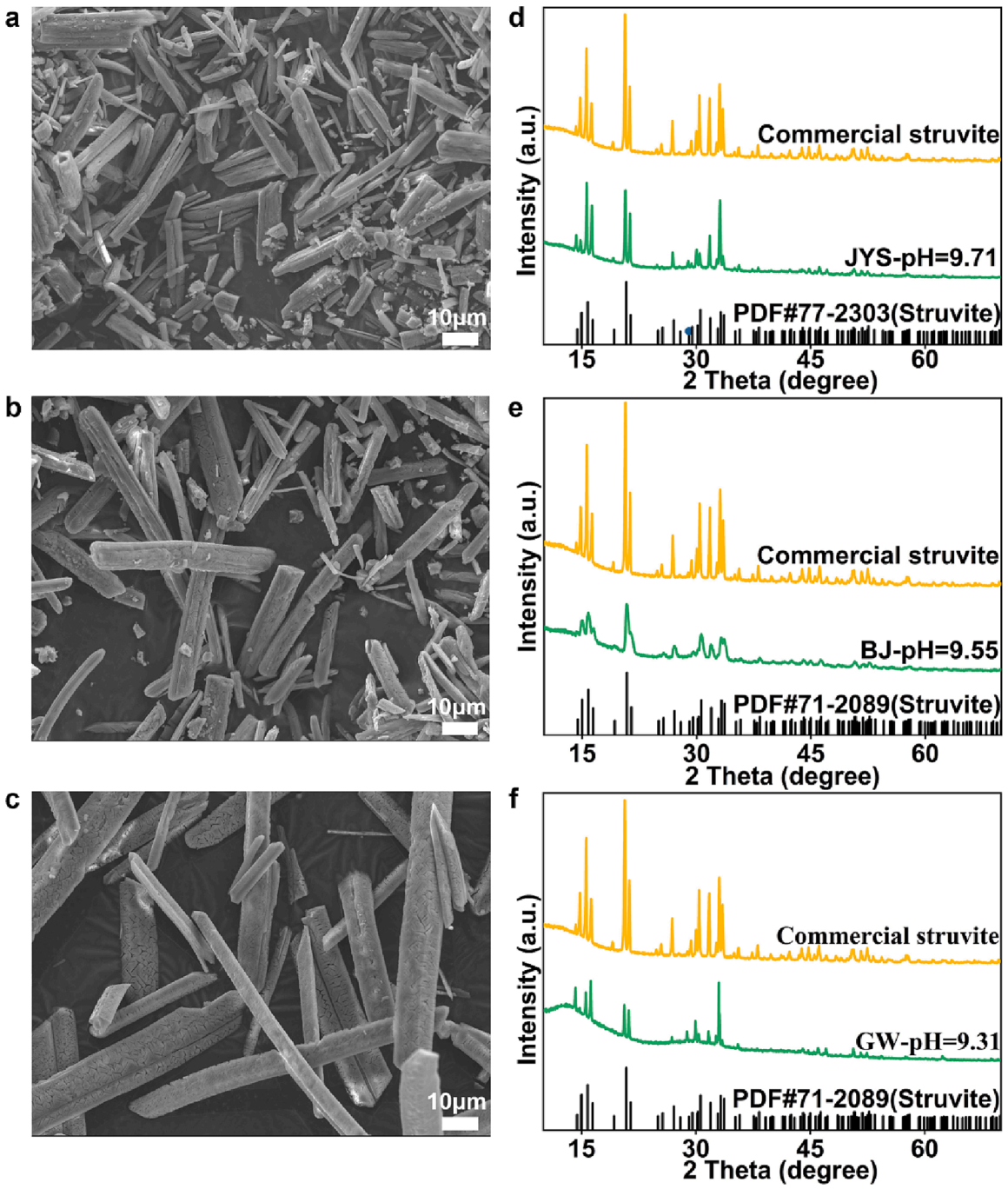

Fig. 6. Morphology and XRD patterns of MAP made of PG JYS-(a), (d). BJ-(b), (e). GW-(c), (f).

within JYS, GW, and BJ leachates can all reach a desorption equilibrium status within 1 h. A phosphorous recycling efficiency of 93.00 ± 3.76%, 97.98 ± 2.47%, and 87.17 ± 1.01%, has been achieved within 0–1 h at this stage, which indicated that the desorption of the ZrO_2 membrane occurred rapidly. As shown in Table 1, more than 92% of the phosphate anions on ZrO_2 membrane can be desorbed with 1 M NaOH. 525.1 mg/L, 358.0 mg/L和592.5 mg/L enriched phosphate solution can be obtained from JYS, GW and BJ respectively by integrated desorption and enrichment techniques. Minor impurities like F, S, and Ca were also presented in the eluent, which will not affect the subsequent phosphorus recovery. Moreover, the membrane can be regenerated and reused for phosphorus adsorption for multiple cycles with good adsorption efficiency, as shown in Fig. 5b.

3.4. Struvite crystallization

With the obtained high-concentration phosphorus anions elute, the struvite crystallization process becomes straightforward. The chemical equation on Struvite crystallization is given in Eq. (1) [28]. It is well-known that the crystallization of struvite from a solution is heavily affected by factors such as pH, composition ratio, temperature, composition, and time. Among all the parameters under the struvite crystallization process, with the defined concentrations of phosphorus anions solution at room temperature, the most critical parameter is the pH [29].

$$PO_4^{3-} + Mg^{2+} + NH_4^{+} + 6H_2O \rightarrow MgNH_4PO_4{\cdot}6H_2O \quad (1).$$

In order to understand the effects of pH, we carefully evaluate the pH effects within the artificial solutions with similar phosphate anions

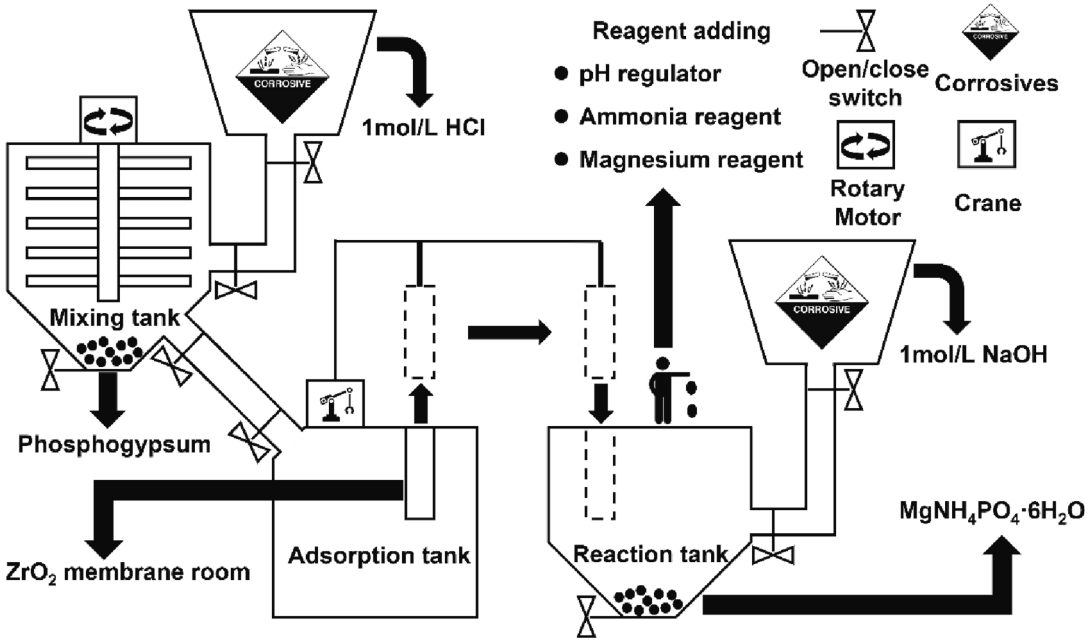

Fig. 7. Working principle of phosphorus recovery device from PG.

concentrations. It can be found that the phosphorus recovery efficiency is positively correlated with pH. When pH = 11.02, the phosphorus removal ratio reached a maximum value of 98.26%. When pH = 9.22–9.76, a large-sized dendritic struvite crystal with high purity, as shown in Fig. S7-8, was produced in artificial wastewater. The morphology and composition are similar to the commercial struvite (Fig. S9). Under this circumstance, the phosphorus removal ratio is 96.85%-97.55% (Fig. S6), which shows that struvite crystallization can recover most of the phosphorus in the solution.

In the PG eluent, the phosphorus removal ratio is positively correlated with the pH when the pH $\leq$ 10.08; while the phosphorus removal ratio is negatively correlated with pH when pH greater than 10.08. At the optimal pH, JYS, BJ, and GW reached the maximum phosphorus removal ratios of 79.36%, 76.55%, and 71.34% at this step, respectively (Fig. S6). The difference in phosphorus removal ratio between the simulated wastewater and eluate may be ascribed to the different initial phosphorus concentrations and impurities, as these parameters also heavily influenced the crystallization process. Compared to the phosphorus recovery rate in other solid wastes [30,31,32], the phosphorus recovery efficiency in PGs is among the highest, which indicates that phosphorus recovery from PG leachate is more feasible and efficient. In order to produce high-purity struvite and maintain a high phosphorus removal ratio of 79.36%, 73.26% and 66.11%, pH = 9.71, 9.55 and 9.57 were selected as the crystallization conditions of JYS, BJ and GW, respectively. The struvite produced under this condition forms block-like morphology with the highest purity of 89.83% (Fig. 6a-c, Table S4), which is close to the commercial struvite (Fig. 6d-f). The heavy metal content in MAP products is lower than the fertilizer limit (Table S5), which shows great potential to be used as raw material or agricultural fertilizer [33,34].

3.5. Environmental impact and economic analysis

PG leachate contains a large number of soluble phosphorus ions, which will cause severe phosphorus pollution if discharged arbitrarily. Recovering phosphate from leachate to prepare slow-release struvite fertilizer will not only help to eradicate the phosphorus pollution problem but also create substantial economic benefits. Initiated from the understanding of PG leachate, the high-efficiency phosphorus recovery process designed in this work can achieve highly efficient phosphorus pollutant removal and MAP recovery. An integrated recovery device with basic working principles can be proposed for futural practical phosphorous recovery from PG leachate, as illustrated in Fig. 7. The products recovered from the reaction vessel device can be sold as agricultural slow-release fertilizer or raw materials for battery fabrication. Huge environmental and economic benefits are expected via this process.

The overall phosphorus recovery efficiency depends on the step efficiencies in the four stepwise processes: phosphorus extraction from PG, phosphorus adsorption with ZrO_2 membrane, membrane desorption, and struvite crystallization. It is unavoidable that there is a recovery rate loss in each step. Here, the overall phosphorus recovery efficiency is calculated by multiplying the efficiency in the four stages. It shows that a recovery efficiency of 59.36%, 49.60% and 55.68% has been achieved for the PGs of JYS, BJ and GW, respectively. With the PG from JYS, the highest phosphorus recovery efficiency of 59.36% has been achieved. This process can recover most of the soluble phosphorus. Meanwhile, the unrecovered phosphorus in the wastewater can be recycled for future leaching process, so that the environmental hazardous effects will be minimized. Taking JYS as an example, theoretically, 41.67 kg of struvite can be produced by recycling the phosphorus from 1 m^3 of PG. As the international price for struvite is 1,885 $/t [35], which suggests that the overall profit of MAP from PG are 1.13$/ m^3 considering the cost of chemicals, water, electricity, and labor (Table S6). The calculation details are documented in Text S4. JYS PG stock is about 3,800 m^3, which will generate a profit of 43 million US dollars, and there is a billion-dollar market worldwide.

4. Conclusion

This work systematically studies a new comprehensive process for phosphorus recovery from PG leachate by integrating ZrO_2 membrane-triggered adsorption with the struvite crystallization mechanisms. High-purity struvite has been achieved via these processes. More than 89.23% of the phosphorus anions in the PG leachate can be recovered via membrane-triggered adsorption, while an overall phosphorus recovery efficiency of 59.36% can be achieved via the integrated process. The obtained fine struvite product is of high purity, with $NH_4MgPO_4{\cdot}6H_2O$ weight ratio of up to 89.83%, which shows great potential to be used as a slow-release fertilizer. The novel strategy

developed here demonstrates a green and sustainable pathway toward phosphorus recovery from the PG or PG-polluted groundwater or surface water leachate, which could be applied to practical phosphorus recovery and struvite fertilizer production. Although field production of struvite needs to be carried out in the near future, the novel strategy developed here shows excellent environmental and economic benefits toward phosphorus recovery. We expect that the commercialization of this strategy will shed light on the emergency PG pollution control in the Yangtze River upstream area, which is of great importance to the ecological preservation.

Declaration of Competing Interest

The authors declare that they have no known competing financial interests or personal relationships that could have appeared to influence the work reported in this paper.

Data availability

Data will be made available on request.

Acknowledgments

This study was funded jointly by the National Key R&D Plan of China (2021YFC3201000), the Strategic Priority Research Program of CAS (No. XDB40020400), the Chinese NSF project (No. 41977296, 42277253), the Central Leading Local Science and Technology Development Fund Project (20214028), the Science and Technology Service Plan of CAS (KFJSTSQYZD202124001), the Opening Fund of the State Key Laboratory of Environmental Geochemistry (SKLEG2023213) and the Youth Innovation Promotion Association CAS (No. 2019389).

Appendix A. Supplementary data

Supplementary data to this article can be found online at https://doi.org/10.1016/j.cej.2023.144310.

References

[1] T. Mardamootoo, K. Ng Kee Kwong, C.J.S.T. Du Preez, History of phosphorus fertilizer usage and its impact on the agronomic phosphorus status of sugarcane soils in Mauritius, 12 (2010) 91-97.
[2] D.P. Van Vuuren, A.F. Bouwman, A.H.W. Beusen, Phosphorus demand for the 1970–2100 period: A scenario analysis of resource depletion, Glob. Environ. Chang. 20 (3) (2010) 428–439, https://doi.org/10.1016/j.gloenvcha.2010.04.004.
[3] A. Yesigat, A. Worku, A. Mekonnen, W. Bae, G.L. Feyisa, S. Gatew, J.L. Han, W. Liu, A. Wang, A. Guadie, Phosphorus recovery as K-struvite from a waste stream: A review of influencing factors, advantages, disadvantages and challenges, Environ. Res. 214 (Pt 3) (2022), 114086, https://doi.org/10.1016/j.envres.2022.114086.
[4] H. Tayibi, M. Choura, F.A. Lopez, F.J. Alguacil, A. Lopez-Delgado, Environmental impact and management of phosphogypsum, J. Environ. Manage. 90 (8) (2009) 2377–2386, https://doi.org/10.1016/j.jenvman.2009.03.007.
[5] M. Contreras, S.R. Teixeira, G.T.A. Santos, M.J. Gázquez, M. Romero, J.P. Bolívar, Influence of the addition of phosphogypsum on some properties of ceramic tiles, Constr. Build. Mater. 175 (2018) 588–600, https://doi.org/10.1016/j.conbuildmat.2018.04.131.
[6] J. Yang, W. Liu, L. Zhang, B. Xiao, Preparation of load-bearing building materials from autoclaved phosphogypsum, Constr. Build. Mater. 23 (2) (2009) 687–693, https://doi.org/10.1016/j.conbuildmat.2008.02.011.
[7] A.M. Rashad, Phosphogypsum as a construction material, J. Clean. Prod. 166 (2017) 732–743, https://doi.org/10.1016/j.jclepro.2017.08.049.
[8] R. El Zrelli, L. Rabaoui, H. Abda, N. Daghbouj, R. Perez-Lopez, S. Castet, T. Aigouy, N. Bejaoui, P. Courjault-Rade, Characterization of the role of phosphogypsum foam in the transport of metals and radionuclides in the Southern Mediterranean Sea, J. Hazard. Mater. 363 (2019) 258–267, https://doi.org/10.1016/j.jhazmat.2018.09.083.
[9] R. Perez-Lopez, F. Macias, C.R. Canovas, A.M. Sarmiento, S.M. Perez-Moreno, Pollutant flows from a phosphogypsum disposal area to an estuarine environment: An insight from geochemical signatures, Sci. Total Environ. 553 (2016) 42–51, https://doi.org/10.1016/j.scitotenv.2016.02.070.
[10] Y. Qin, M.A. Yingqun, L. Wang, B. Zheng, C. Ren, H. Tong, H.J.R.o.E.S. Wang, Pollution of the Total Phosphorus in the Yangtze River Basin:Distribution Characteristics,Source and Control Strategy, (2018).
[11] O. Hentati, N. Abrantes, A.L. Caetano, S. Bouguerra, F. Goncalves, J. Rombke, R. Pereira, Phosphogypsum as a soil fertilizer: Ecotoxicity of amended soil and elutriates to bacteria, invertebrates, algae and plants, J. Hazard. Mater. 294 (2015) 80–89, https://doi.org/10.1016/j.jhazmat.2015.03.034.
[12] M. Renteria-Villalobos, I. Vioque, J. Mantero, G. Manjon, Radiological, chemical and morphological characterizations of phosphate rock and phosphogypsum from phosphoric acid factories in SW Spain, J. Hazard. Mater. 181 (1–3) (2010) 193–203, https://doi.org/10.1016/j.jhazmat.2010.04.116.
[13] J. Xu, L. Fan, Y. Xie, G. Wu, Recycling-equilibrium strategy for phosphogypsum pollution control in phosphate fertilizer plants, J. Clean. Prod. 215 (2019) 175–197, https://doi.org/10.1016/j.jclepro.2018.12.236.
[14] S.K. Ramasahayam, L. Guzman, G. Gunawan, T. Viswanathan, A Comprehensive Review of Phosphorus Removal Technologies and Processes, J. Macromol. Sci. A 51 (6) (2014) 538–545, https://doi.org/10.1080/10601325.2014.906271.
[15] L.A. Rodrigues, L.J. Maschio, L.d.S.C. Coppio, G.P. Thim, M.L.C. Pinto da Silva, Adsorption of phosphate from aqueous solution by hydrous zirconium oxide, Environ Technol 33(10–12) 33 (12) (2012) 1345–1351.
[16] J. Lin, Y. Zhan, H. Wang, M. Chu, C. Wang, Y. He, X. Wang, Effect of calcium ion on phosphate adsorption onto hydrous zirconium oxide, Chem. Eng. J. 309 (2017) 118–129, https://doi.org/10.1016/j.cej.2016.10.001.
[17] L. Delgadillo-Velasco, V. Hernández-Montoya, N.A. Rangel-Vázquez, F. J. Cervantes, M.A. Montes-Morán, M.D.R. Moreno-Virgen, M.d.R. Moreno-Virgen, Screening of commercial sorbents for the removal of phosphates from water and modeling by molecular simulation, J. Mol. Liq. 262 (2018) 443–450.
[18] S. Ding, D. Xu, Q. Sun, H. Yin, C.J.E.s. Zhang, technology, Measurement of dissolved reactive phosphorus using the diffusive gradients in thin films technique with a high-capacity binding phase, 44(21) (2010) 8169-8174.
[19] J. Murphy, J.P.J.A.c.a. Riley, A modified single solution method for the determination of phosphate in natural waters, 27 (1962) 31-36.
[20] M. Walawalkar, C.K. Nichol, G. Azimi, Process investigation of the acid leaching of rare earth elements from phosphogypsum using HCl, HNO3, and H2SO4, Hydrometall. 166 (2016) 195–204, https://doi.org/10.1016/j.hydromet.2016.06.008.
[21] J. Lin, S. He, X. Wang, H. Zhang, Y. Zhan, Removal of phosphate from aqueous solution by a novel Mg(OH)2/ZrO2 composite: Adsorption behavior and mechanism, Colloids Surf A Physicochem Eng Asp 561 (2019) 301–314, https://doi.org/10.1016/j.colsurfa.2018.11.001.
[22] X. Lin, Y. Xie, H. Lu, Y. Xin, R. Altaf, S. Zhu, D. Liu, Facile preparation of dual La-Zr modified magnetite adsorbents for efficient and selective phosphorus recovery, Chem. Eng. J. 413 (2021) 127530.
[23] F. Long, J.-L. Gong, G.-M. Zeng, L. Chen, X.-Y. Wang, J.-H. Deng, Q.-Y. Niu, H.-Y. Zhang, X.-R. Zhang, Removal of phosphate from aqueous solution by magnetic Fe–Zr binary oxide, Chem. Eng. J. 171 (2) (2011) 448–455, https://doi.org/10.1016/j.cej.2011.03.102.
[24] M. Li, J. Liu, Y. Xu, G. Qian, Phosphate adsorption on metal oxides and metal hydroxides: A comparative review, Environ. Rev. 24 (3) (2016) 319–332, https://doi.org/10.1139/er-2015-0080.
[25] Y.H. Magdy, H. Altaher, Kinetic analysis of the adsorption of dyes from high strength wastewater on cement kiln dust, J. Environ. Chem. Eng. 6 (1) (2018) 834–841, https://doi.org/10.1016/j.jece.2018.01.009.
[26] B. Wu, J. Wan, Y. Zhang, B. Pan, I.M.C. Lo, Selective phosphate removal from water and wastewater using sorption: process fundamentals and removal mechanisms, Environ. Sci. Tech. 54 (1) (2020) 50–66, https://doi.org/10.1021/acs.est.9b05569.
[27] E.J. Elzinga, D.L. Sparks, Phosphate adsorption onto hematite: an in situ ATR-FTIR investigation of the effects of pH and loading level on the mode of phosphate surface complexation, J. Colloid Interface Sci. 308 (1) (2007) 53–70, https://doi.org/10.1016/j.jcis.2006.12.061.
[28] X. Liu, Y. Wang, J. Chang, A review on the incorporation and potential mechanism of heavy metals on the recovered struvite from wastewater, Water Res. 207 (2021), 117823, https://doi.org/10.1016/j.watres.2021.117823.
[29] K.S. Le Corre, E. Valsami-Jones, P. Hobbs, S.A.J.C.R.i.E.S. Parsons, Technology, Phosphorus recovery from wastewater by struvite crystallization: A review, 39(6) (2009) 433-477.
[30] N. Marti, L. Pastor, A. Bouzas, J. Ferrer, A. Seco, Phosphorus recovery by struvite crystallization in WWTPs: influence of the sludge treatment line operation, Water Res. 44 (7) (2010) 2371–2379, https://doi.org/10.1016/j.watres.2009.12.043.
[31] S. Liang, H. Chen, X. Zeng, Z. Li, W. Yu, K. Xiao, J. Hu, H. Hou, B. Liu, S. Tao, J. Yang, A comparison between sulfuric acid and oxalic acid leaching with subsequent purification and precipitation for phosphorus recovery from sewage sludge incineration ash, Water Res. 159 (2019) 242–251, https://doi.org/10.1016/j.watres.2019.05.022.
[32] H. Dai, H. Zhang, Y. Sun, H.N. Abbasi, Z. Guo, L. Chen, Y. Chen, X. Wang, S. Zhang, An integrated process for struvite recovery and nutrient removal from ship domestic sewage, Water Res. 228 (Pt B) (2023), 119381, https://doi.org/10.1016/j.watres.2022.119381.
[33] H.-D. Ryu, S.-I. Lee, Struvite recovery from swine wastewater and its assessment as a fertilizer, Environ. Eng. Res. 21 (1) (2016) 29–35, https://doi.org/10.4491/eer.2015.066.
[34] J.J. Mortvedt, Heavy metal contaminants in inorganic and organic fertilizers, 43(1-3) (1996) 55-61. doi: 10.1007/978-94-009-1586-2_2.
[35] P. Achilleos, K.R. Roberts, I.D. Williams, Struvite precipitation within wastewater treatment: A problem or a circular economy opportunity? Heliyon 8 (7) (2022) e09862, https://doi.org/10.1016/j.heliyon.2022.e09862.